The EMBO Journal Vol.18 No.19 pp.5264–5273, 1999

Deletion of the ryanodine receptor type 3 (RyR3) impairs forms of synaptic plasticity and spatial learning

Detlef Balschun, David P.Wolfer[1], Federica Bertocchini[2], Virginia Barone[2], Antonio Conti[2], Werner Zuschratter, Ludwig Missiaen[3], Hans-Peter Lipp[1], J.Uwe Frey and Vincenzo Sorrentino[2,4,5]

Leibniz-Institute for Neurobiology, Magdeburg, Germany, [1]Institute of Anatomy, University of Zurich, Switzerland, [2]DIBIT, Istituto Scientifico San Raffaele, via Olgettina 58, I-20132 Milano, Italy, [3]Department of Physiology, Katholieke Universiteit Leuven, Belgium and [4]Department of Biomedical Sciences, University of Siena, Italy

[5]Corresponding author
e-mail: sorrentino.vincenzo@hsr.it

Deletion of the ryanodine receptor type 3 (RyR3) results in specific changes in hippocampal synaptic plasticity, without affecting hippocampal morphology, basal synaptic transmission or presynaptic function. Robust long-term potentiation (LTP) induced by repeated, strong tetanization in the CA1 region and in the dentate gyrus was unaltered in hippocampal slices *in vitro*, whereas weak forms of plasticity generated by either a single weak tetanization or depotentiation of a robust LTP were impaired. These distinct physiological deficits were paralleled by a reduced flexibility in re-learning a new target in the water-maze. In contrast, learning performance in the acquisition phase and during probe trial did not differ between the mutants and their wild-type littermates. In the open-field, RyR3$^{-/-}$ mice displayed a normal exploration and habituation, but had an increased speed of locomotion and a mild tendency to circular running. The observed physiological and behavioral effects implicate RyR3-mediated Ca^{2+} release in the intracellular processes underlying spatial learning and hippocampal synaptic plasticity.

Keywords: behavior/calcium release channels/ryanodine receptor type 3/spatial learning/synaptic plasticity

Introduction

A considerable amount of evidence from a variety of experimental models suggests that long-lasting changes of synaptic plasticity as well as the formation of long-term memory require at least two major cellular events: an initial elevation of the intracellular calcium concentration $[Ca^{2+}]_i$ and, subsequently, a *de novo* synthesis of certain proteins, mediated by different second messenger cascades (Davis and Squire, 1984; Goelet *et al*., 1986; Malenka *et al*., 1988, 1992; Lisman, 1989; Matthies, 1989; Artola and Singer, 1993; Bootman and Berridge, 1995; Cummings *et al*., 1996; Rosenzweig, 1996; Tsumoto and Yasuda, 1996; Frey and Morris 1997; Alkon *et al*., 1998). Beyond the influx of Ca^{2+} via *N*-methyl-D-aspartate receptors (NMDARs) and voltage-dependent calcium channels (VDCCs) (Grover and Teyler 1990, 1994; Bliss and Collingridge, 1993), the release of Ca^{2+} from intracellular stores located in the endoplasmic reticulum provides a main source of intracellular Ca^{2+}, which has been implicated in several forms of synaptic plasticity and memory formation (Xu and Krnjevic, 1990; Kohda *et al*., 1995; O'Mara *et al*., 1995; Frenguelli *et al*., 1996; Reyes and Stanton, 1996; Wang *et al*., 1996, 1997; Alkon *et al*., 1998; Wilsch *et al*., 1998). Although both types of endoplasmic calcium release channels—inositol 1,4,5-trisphosphate (InsP3) receptors and ryanodine receptors (RyRs)—were found to be involved in neuronal plasticity, RyRs apparently possess a particular importance: (i) they amplify Ca^{2+} signals initiated by other extracellular and intracellular Ca^{2+} sources (Berridge, 1998; Reyes-Harde *et al*., 1999); (ii) they are tightly functionally coupled to the influx of extracellular Ca^{2+} through L-type VDCCs (Chavis *et al*., 1996); and (iii) RyRs but not InsP3 receptors appear to modulate cellular protein synthesis (Alcazar *et al*., 1997).

To date, three isoforms of RyRs (RyR1, RyR2 and RyR3) are known, which are all expressed in the central nervous system (CNS) (Furuichi *et al*., 1994; Giannini *et al*., 1995). In the brain, RyR2 is expressed at robust levels while RyR1 and RyR3 contribute only a small fraction of total RyRs in neurons. It is interesting to note that the three RyR isoforms differ in their pattern of expression in distinct areas of the brain (Furuichi *et al*., 1994; Giannini *et al*., 1995). For instance, RyR1 is preferentially expressed in Purkinjes cells in contrast with RyR2, which is expressed in the cerebellar granule cells as well as in many other areas of the brain. RyR3 is preferentially found in the hippocampal CA1 pyramidal cell layer, the caudate/putamen, the olfactory bulb and olfactory tubercle. In parallel to these preferential sites of expression, in many areas of the brain more than one RyR isoform is observed. Immunohistochemical studies, performed with antibodies that recognize more than one RyR isoform (global RyR staining), have revealed that the localization of RyRs may often coincide with that of the InsP3 receptors in most regions of the brain, while in others a differential localization can be observed (Sharp *et al*., 1993). RyR immunostaining has been observed in cell bodies, axons, dendrites, spines and dendritic shafts (Sharp *et al*., 1993; Berridge, 1998).

Why multiple RyR isoforms exist in numerous neurons and how these isoforms participate and interact in neuronal function is currently not understood. The development of RyR3 gene knockout mice has provided initial evidence for the involvement of RyR3 channels in muscle contraction. In neonatal skeletal muscles, where RyR3 is expressed with a relative abundance (Conti *et al*., 1996; Bertocchini *et al*., 1997; Flucher *et al*., 1999), knockout of RyR3

reduces the amplitude of the twitch and unfused tetani in electrically stimulated muscles. Furthermore, it reduces contracture induced by caffeine (Bertocchini *et al*., 1997). Since RyR3 levels in skeletal muscles are only a fraction of those seen in total RyR channels, it has been proposed that RyR3 channels may provide a robust amplificatory component in conjunction with the voltage-activated RyR1 channels (Bertocchini *et al*., 1997; Sonnleitner *et al*., 1998; Sorrentino and Reggiani, 1999).

To examine the functional role of the RyR3 gene product in the CNS, mutant mice homozygous for a non-functional allele of the RyR3 gene were studied at the morphological, physiological and behavioral levels. Because of the relatively high expression of RyR3 in the hippocampus (Furuichi *et al*., 1994; Giannini *et al*., 1995), studies were focused on this brain region.

RyR3 knockout mice developed normally and showed no obvious morphological alteration in the hippocampus. Likewise, long-term potentiation (LTP) generated by a strong, 3-fold tetanization and spatial learning in the Morris water-maze did not differ between mutant and control animals. In contrast, weak LTP, depotentiation (DP) and spatial re-learning were markedly changed by RyR3 deletion. Thus, RyR3 channels seem to play a distinct role in certain types of hippocampal synaptic plasticity and spatial learning.

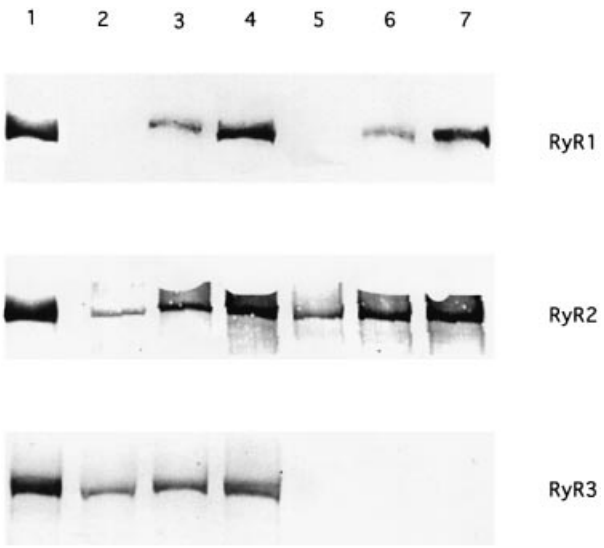

Fig. 1. Developmental expression of the RyR isoforms in brain. Western blot analysis of RyR isoforms in microsomal proteins from brain of 2-day-old (lanes 2 and 5), 15-day-old (lanes 3 and 6) and adult mice (lanes 4 and 7). Lanes 2, 3 and 4 refer to normal mice, while lanes 5, 6 and 7 refer to RyR3-knockout; 50, 2 and 20 μg of microsomal vesicles were loaded for RyR1, RyR2 and RyR3 immunodetection, respectively. Lane 1 contains control microsomes prepared from skeletal muscle, cardiac muscle and diaphragm muscle used as control for RyR1, RyR2 and RyR3 immunodetection, respectively.

Results

Morphological characterization and RyR isoform expression in the brain of RyR3 knockout mice

In wild-type animals, the three isoforms of RyRs are expressed in the CNS, where their levels increase between late embryonic stages of development and 60 days after birth (Figure 1). Knockout of the RyR3 gene did not affect the expression level of the RyR1 and RyR2 isoforms in the brain (Figure 1). In a separate set of experiments, the levels of the three isoforms of InsP3 receptors in the brain of RyR3 knockout mice were analyzed using isoform-specific antibodies. No difference with respect to normal mice was observed (data not shown). To assess the morphological development of RyR3 mutants and their wild-type counterparts, we used Nissl staining and antibodies towards the calcium-binding proteins parvalbumin, calbindin D28K and calretinin that indicate specific subtypes of interneurons and principal cells. S100β served as a glial marker. As shown in Figure 2, RyR3 mutant mice did not display obvious alterations in the number, distribution or morphology of hippocampal neurons or glial cells as compared with their wild-type counterparts. Likewise, the distribution patterns of parvalbumin, calbindin and calretinin immunoreactivity in mutant mice resembled those of wild-type controls (Figure 3).

LTP analysis in CA1 and dentate gyrus of RyR3 knockout mice

Previous studies have revealed a relative abundance of RyR3 in neurons of the hippocampus (Furuichi *et al*., 1994; Giannini *et al*., 1995). These observations are suggestive of a functional role of RyR3 channels in hippocampal Ca^{2+} signaling. The dynamics of intraneuronal Ca^{2+} $[Ca^{2+}]_i$ have been found to play a critical role during the induction of plastic synaptic changes in the hippocampus, since they determine the type and properties of synaptic changes that are induced [e.g. LTP and LTD (long-term depression); Lisman, 1989; Artola and Singer, 1993; Cummings *et al*., 1996; Tsumoto and Yasuda, 1996; but see Neveu and Zucker, 1996]. Therefore, we examined whether hippocampal synaptic plasticity was altered in the RyR3 knockout mice. In particular, we studied LTP, which is thought to mediate processes of learning and memory formation at the cellular level (Bliss and Collingridge, 1993). In a first set of experiments, robust LTP (lasting for at least 6 h) was induced either in the hippocampal CA1 region or in the dentate gyrus by a repeated, strong tetanization protocol (Figures 4A–C and 5A). In the two regions, no statistical differences could be detected between RyR3 knockout and wild-type control mice, neither in LTP induction as expressed by the degree of potentiation 1 min after the third tetanus [dentate gyrus: $RyR3^{+/+}$: 206.4 ± 16.3 (% change ± SEM), $n = 7$; $RyR3^{-/-}$ 212.1 ± 14.5, $n = 6$; CA1: $RyR3^{+/+}$: 188.8 ± 33.1, $n = 5$; $RyR3^{-/-}$: 183.5 ± 27.2, $n = 5$], nor in the maintenance of LTP as evaluated by the potentiation 6 h after tetanization (dentate gyrus: $RyR3^{+/+}$, 137.05 ± 8.3; $RyR3^{-/-}$, 143.2 ± 11.4; CA1: $RyR3^{+/+}$, 151.3 ± 11.7; $RyR3^{-/-}$, 152.4 ± 20.1).

The lack of an effect of RyR3 receptor deletion on robust LTP could be caused by the strong induction protocol, which activates cellular processes that provide the cell with a large amount of extracellular calcium (e.g. calcium influx via voltage-dependent calcium channels, NMDARs, etc.). We therefore tested whether an LTP generated by a weaker tetanization protocol would be affected, reasoning that a potentiation induced by such a protocol could be more susceptible to a diminution of $[Ca^{2+}]_i$ elevation during tetanization, as can be anticipated

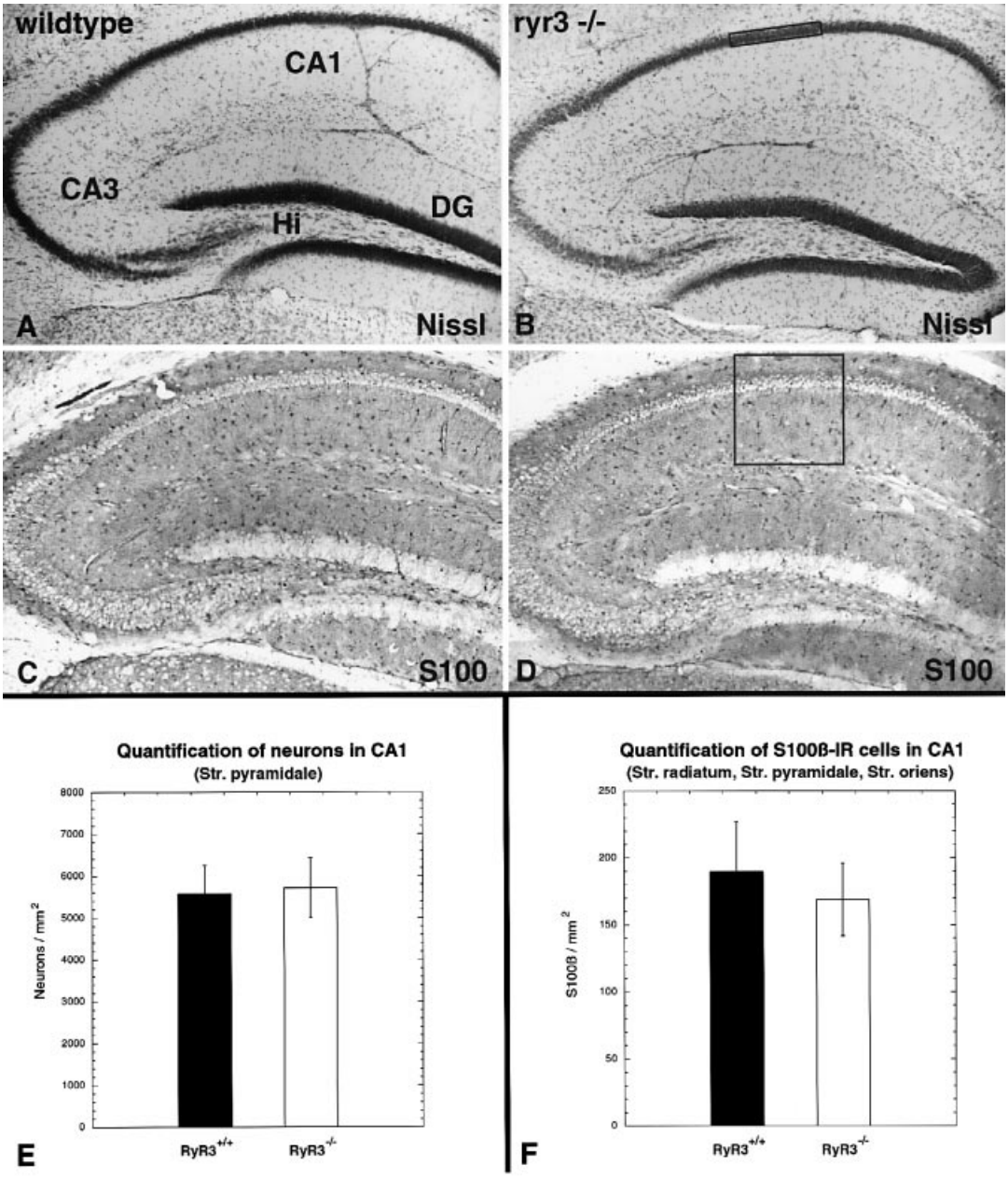

Fig. 2. (**A** and **B**) Comparison of Nissl- and (**C** and **D**) S100β-stained sections from RyR3 knockout and wild-type mice. Deletion of RyR3 did not change the distribution, number or size of neurons or S100β-immunoreactive glial cells in the hippocampal formation. Quantification of (**E**) neurons and (**F**) S100β-IR glial cells revealed no significant difference between the two groups in the analyzed areas (see box in B, D). Columns indicate mean values ± standard deviation of $n = 3$ animals/group (with $n = 15$ sections/animal in the case of Nissl-stained sections and $n = 5$ sections/animal in the case of S100β-IR glial cells).

in RyR3 knockout mice. In accordance with these considerations, mutant mice tended to have a lower initial amplitude of potentiation (154.1 ± 8.7, $n = 7$, compared with 174.5 ± 4.7, $n = 5$, of controls) and, more importantly, were impaired in LTP maintenance (Figure 5B–D). LTP in RyR3 knockout mice decayed within 30 min (Figure 5B), whereas wild-type mice still displayed a significant potentiation after 2 h (129.4 ± 13.6). The difference between RyR3 knockout mice and controls was highly statistically significant.

Depotentiation in the dentate gyrus

Since these results indicated that RyR3 is distinctly involved in certain types of LTP induced by weak tetanization protocols, we examined whether other forms of synaptic plasticity were also affected. Since homosynaptic LTD can not be induced in the medial perforant path of adult rodents (Doyere *et al*., 1997), we studied DP in this structure. DP assigns the reversal of potentiation evoked by low-frequency stimulation shortly after induction of LTP (Barrionuevo *et al*., 1980; Stäubli and Chun, 1996; Wagner and Alger, 1996). It was reported to share several biochemical characteristics with LTD (Wagner and Alger, 1996). In both RyR3 knockout mice and their wild-type controls, a single tetanus at 100 Hz (1 s) caused a significant potentiation (Figure 4D–F). In RyR3 knockout mice, application of a 2 min train of low-frequency

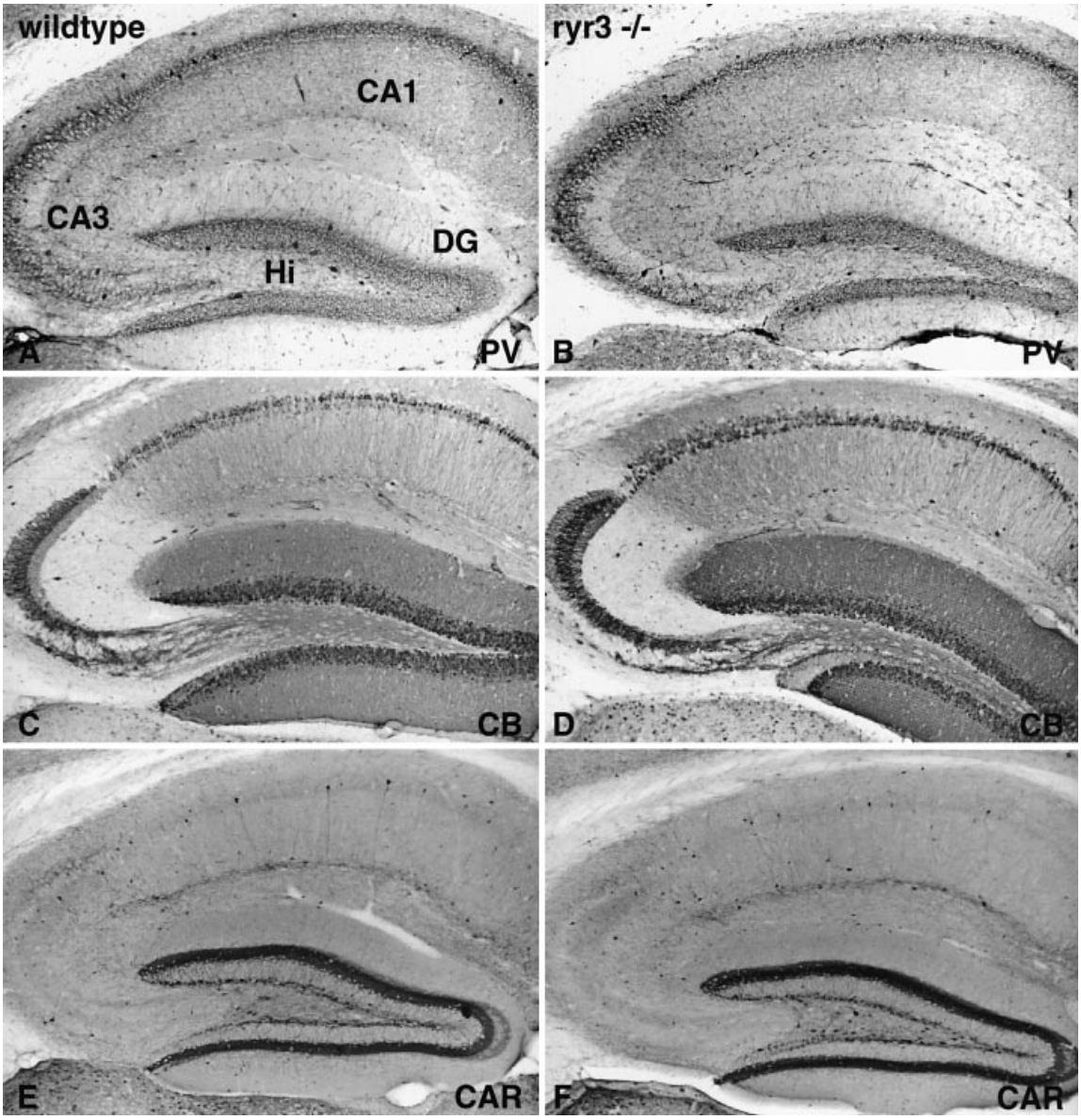

Fig. 3. The immunocytochemical detection of cell-type-specific markers for the calcium-binding proteins (**A** and **B**) parvalbumin, (**C** and **D**) calbindin D28K and (**E** and **F**) calretinin revealed similar staining patterns of neurons in wild-type (A, C and E) and mutant mice (B, D and F).

stimulation, 5 min after induction of LTP, resulted consistently in a DP of field excitatory postsynaptic potential (fEPSP) slope to intermediate levels significantly different from potentiation and baseline. Thereafter, the residual potentiation of the RyR3 knockout mice showed a further decay which became indistinguishable from baseline levels 30 min after DP (Figure 4E and F). In contrast, wild-type controls remained at the residual potentiated level until the end of recording. This difference in the maintenance of the residual potentiation was not due to an altered basal synaptic function in RyR3 mutants as shown by input–output (I/O) curves (Figure 4G).

Next, we examined whether paired-pulse depression was affected in RyR3 knockout mice. This presynaptically governed form of short-term plasticity is observed when two identical stimuli are delivered to homosynaptic afferent fibers in rapid succession (Anderson, 1960; Curtis and Eccles, 1960). Over the whole range of interpulse intervals (10–500 ms), virtually no difference was observed in paired-pulse depression between RyR3-deficient mice and controls (Figure 4H).

Behavior and learning in RyR3 knockout mice

The specific effects of RyR3 deletion on synaptic plasticity suggest a role of RyR3 in hippocampus-dependent learning and behavior. Since the performance in a learning task may be confounded by side-effects of gene deletion on general behavior, we first analyzed spontaneous activity in an open-field test. Mutant mice travelled an 18% longer distance (Figure 6A) due to greater speed of locomotion. Both effects were more pronounced during the first day. The faster locomotion of RyR3 mutant mice was associated with an increased tendency of circular running (Figure 6B), which may be interpreted as a mild motor stereotypy. In contrast, mutants showed normal habituation of activity, and the time spent resting was indistinguishable from controls within-session. There was also no difference with

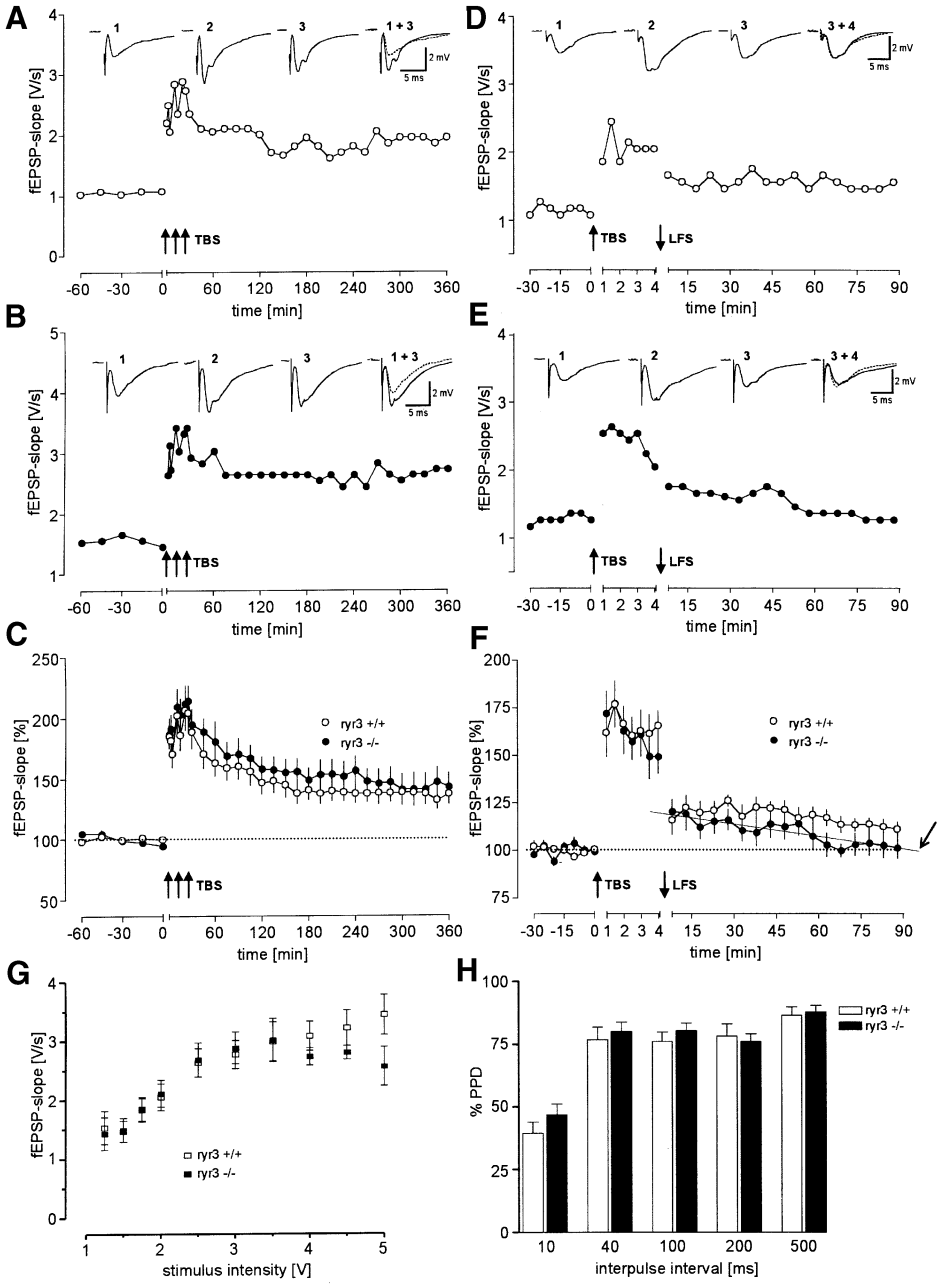

Fig. 4. LTP and DP in the dentate gyrus of RyR3$^{+/+}$ (○) and RyR3$^{-/-}$ (●) mice as determined by the initial slope of the fEPSPs. (A–C) Deletion of RyR3 does not impair robust LTP induced by strong, triple tetanization (TBS, theta-burst stimulation, indicated by arrows) in the dentate gyrus. (**A** and **B**) Examples of LTP in (A) a wild-type and (B) a mutant mouse. The insets represent analog traces, taken (1) during baseline recording, (2) immediately after tetanization and (3) 6 h post-tetanus. Note the increased slope of the fEPSP after tetanization. The superimposed traces (1 + 3) indicate the remaining potentiation after 6 h. (**C**) Average values (means ± SEM) calculated as a percentage of baseline measures (RyR3$^{+/+}$, $n = 8$; RyR3$^{-/-}$, $n = 6$). (D–F) Deletion of RyR3 affects DP in the dentate gyrus. (**D** and **E**) Individual examples of DP in (D) a wild-type and (F) a mutant mouse. Analog traces were taken (1) during baseline recording, (2) immediately after tetanization, (3) immediately after DP and (4) 80 min thereafter. Trace 3 is superimposed on trace 4 (broken line: trace 3) to allow an evaluation of the stability of remaining potentiation after DP. (**F**) Average values (means ± SEM) calculated as percentage of baseline measures. Note the continuous decrease of the fEPSP slope of RyR3$^{-/-}$ ($n = 7$) mice after cessation of low-frequency stimulation (LFS) that is evident by the calculated regression line $y = 120.3–0.23x$ ($P < 0.0002$, Friedman test; RyR3$^{+/+}$, $n = 8$). (**G**) Input–output curves of RyR3-deficient and wild-type control mice. fEPSP slopes were recorded at increasing stimulation intensities until a maximum was attained. There were no significant differences between the two groups. Means ± SEM, RyR3$^{+/+}$, $n = 8$; RyR3$^{-/-}$, $n = 7$. (**H**) Paired-pulse depression (PPD), calculated from the ratio of the second fEPSP slope to the first fEPSP slope. At all interpulse intervals, no significant difference was observed between RyR3$^{-/-}$ and RyR3$^{+/+}$ mice. Means ± SEM are given. RyR3$^{+/+}$, $n = 8$; RyR3$^{-/-}$, $n = 7$.

respect to the amount of time spent in contact with the wall or exploring the center of the arena.

Hippocampus-dependent spatial learning of RyR3 knockout mice was examined in a Morris water-maze test. During an acquisition phase (18 trials) the animals had to learn to use distant cues on the walls to locate an escape platform that was hidden at a constant location. This was followed by a reversal phase (12 trials) during which the cues remained unchanged but the platform was relocated to a new position. Navigation learning during the acquisition

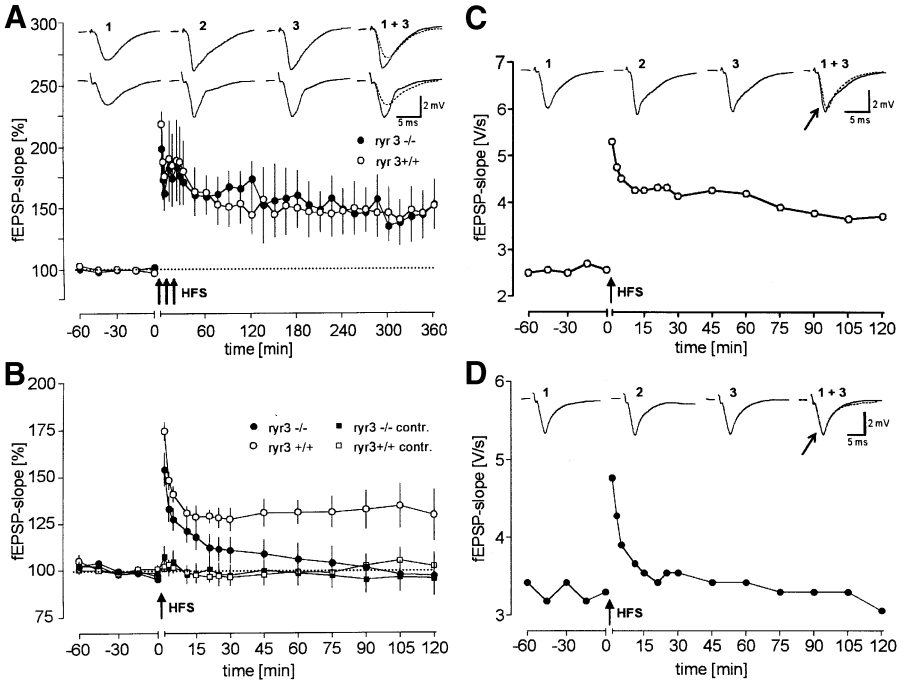

Fig. 5. LTP of the fEPSP in the hippocampal CA1-region of RyR3$^{-/-}$ (●) and RyR3$^{+/+}$ (○) mice. (**A**) Deletion of RyR3 does not deteriorate robust LTP induced by strong, triple tetanization (HFS, high-frequency stimulation) indicated by arrows. The insets represent analog traces of a wild-type (upper row) and a mutant (lower row) mouse, taken (1) during baseline recording, (2) immediately after tetanization and (3) 6 h post-tetanus (RyR3$^{-/-}$, $n = 5$; RyR3$^{+/+}$, $n = 5$). (**B**) LTP induced by a single weak tetanization in the CA1 area is impaired in RyR3$^{-/-}$ ($n = 7$, ●) mice compared with RyR3$^{+/+}$ ($n = 5$, ○; $P < 0.002$, ANOVA with repeated measures). In contrast, RyR3$^{-/-}$ mice (■) show an unchanged baseline transmission of an independent control input (□: RyR3$^{+/+}$ mice). (**C** and **D**) Representative examples of weak LTP in (C) a wild-type and (D) a mutant mouse. The insets represent analog traces taken (1) during baseline recording, (2) immediately after tetanization and (3) 2 h thereafter. The superimposed traces (1 + 3) indicate that in the wild-type animal, but not in the mutant mouse, potentiation is still present at 2 h after tetanization (indicated by an arrow).

phase was normal in RyR3 knockout mice with respect to escape latency (Figure 6C), swim path length and cumulative search error (Gallagher *et al*., 1993). There was also no evidence for increased swim speed or an abnormal circling tendency. Furthermore, RyR3 knockout mice formed a normal spatial memory as assessed by measuring the time spent in the former platform quadrant during the probe trial (first 60 s after relocating the target) and comparing it with the two adjacent quadrants (Figure 6D). During the probe trial, both RyR3 knockout mice and controls also swam more often over the trained goal site than over control sites in the adjacent quadrants. An interesting difference emerged after changing the platform position. Wild-type animals learned the new position very rapidly, taking only two to three trials to reach the performance level they had shown at the end of acquisition (Figure 6C). RyR3 knockout mice, in contrast, needed the full 12 trials to learn the new position, apparently having no advantage with respect to the acquisition phase. Their escape times and swim paths were longer (28 and 14% on average, respectively) than those of wild-type animals, and their cumulative search error was increased by 37%. As during acquisition, they frequently swam along the wall or aimlessly scanned the pool in wide loops. A few mutants that had shown excellent probe trial scores also quite obsessively searched around the previous platform location. The genotype differences with respect to learning and re-learning were statistically significant (see legend to Figure 6).

Discussion

The findings of this study shed new light on the role of RyRs in synaptic and behavioral plasticity. It is generally accepted that the induction of LTP and LTD requires an elevation of intracellular Ca^{2+} concentration in the postsynaptic neuron that is mediated either by channels on the plasma membrane and/or by InsP3 receptors and RyR release channels localized on specialized intracellular Ca^{2+} stores (Lisman, 1989; Malenka *et al*., 1992; Artola and Singer, 1993; Bootman and Berridge, 1995; Cummings *et al*., 1996; Tsumoto and Yasuda, 1996). An accepted model for activation of Ca^{2+} release through RyRs in neurons envisages a Ca^{2+}-induced Ca^{2+} release mechanism where an influx of Ca^{2+} through plasma membrane channels triggers the activation of the RyRs (Berridge, 1998). In addition, a functional coupling between RyRs and L-type Ca^{2+} channels could also be involved in RyR-coupled Ca^{2+} signaling (Chavis *et al*., 1996). A role of RyRs in the induction of LTP and LTD has been supported by a number of experiments all based on the use of pharmacological agents (Xu and Krnjevic, 1990; Kohda *et al*., 1995; O'Mara *et al*., 1995; Reyes and Stanton, 1996; Wang *et al*., 1997). However, these studies did not allow the identification of either the functional contribution of each single isoform or the significance of the expression of multiple RyR isoforms within a single neuron.

In the knockout mice used for our study, the RyR3 isoform was selectively deleted without changing the

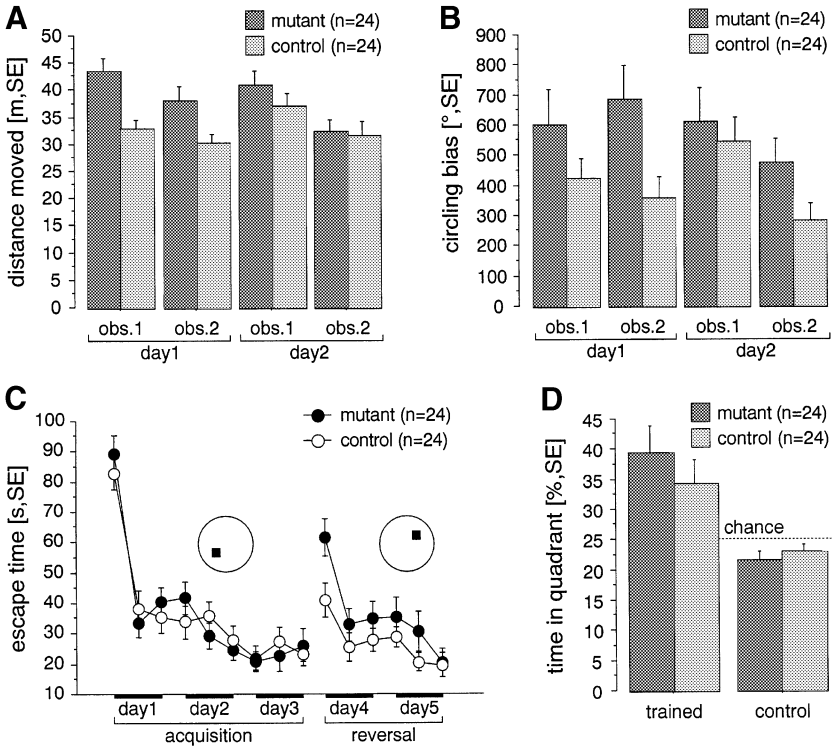

Fig. 6. Behavioral analysis of RyR3 mutant mice: (A and B) spontaneous open-field activity and (C and D) spatial learning in the hidden-platform Morris water-maze. (**A**) Each column represents the distance moved during an open-field observation period of 5 min. During the first day and the first 5 min of the second day, RyR3 mutant mice move a greater distance than controls. (**B**) The increased locomotion of RyR3 mutant mice is associated with an increased tendency of circular running, as shown by an increased circling bias [sum of all counter-clockwise (+) and clockwise (–) direction changes]. (**C**) Escape latency in the hidden-platform water-maze plotted by blocks of two trials. Compared with their wild-type littermates, the water-maze escape performance of RyR3 mutant mice is normal during the acquisition phase (days 1–3), but impaired during relearning of a new platform position in the same pool (reversal phase, days 4–5). Note that this selective mutation effect on the learning of a new platform location (in an otherwise unchanged environment) was confirmed statistically by significant genotype-learning phase interactions (comparing average performance during reversal and acquisition): time F (46, 1) = 6.36, P <0.0152; path F (46, 1) = 7.68, P <0.0080, search error F (46, 1) = 6.31, P <0.0156. Scheffe *post hoc* analysis confirmed the mutation effect on reversal performance (time P <0.0068, path P <0.0009, search error P <0.0055) and confirmed that wild types performed better during reversal than acquisition (time P <0.0076, path P <0.0060, search error P <0.0440), whereas RyR3 knockouts did not (time, path and search error not significant). (**D**) During the probe trial (the first 60 s of reversal), RyR3 knockout mice show intact spatial preference for the trained quadrant.

expression of RyR1 or RyR2, or of the InsP3 receptors. However, one must still consider the possibility that yet undetected changes in other proteins involved in Ca^{2+} homeostasis or in specific cellular structures may have occurred as a consequence of RyR3 deletion. Yet, these mutants represent an ideal model for examining the function of the RyR3 isoform. Whereas RyR3 mutant mice did not show any changes in the cytoarchitectonical distribution patterns of neuronal subtypes in the hippocampus, the electrophysiological studies revealed specific changes of hippocampal synaptic plasticity. In contrast to robust LTP (induced by strong, repeated tetanization), which was affected neither in area CA1 nor in the dentate gyrus, a weaker form of LTP in the CA1 region (induced by weak single tetanization) was impaired. Another form of synaptic plasticity, DP, was altered in the dentate gyrus of RyR3 knockout mice. Interestingly, the magnitude of DP was not changed, but RyR3 knockout mice were impaired in maintaining a residual potentiation, which is indicative of a reset of LTP to a lower level, i.e. a decremental potentiation. According to our experience, such a weaker form of dentate LTP is difficult to accomplish by 'direct' weak tetanization. The changes observed in hippocampal synaptic plasticity are seemingly not a consequence of an altered excitability or a changed presynaptic function, since both I/O-curve and paired-pulse depression (PPD) were identical in mutants and controls. The consistently strong depression observed over the whole range of interpulse intervals corroborates previous findings on PPD in the medial perforant path of the rat (McNaughton, 1982).

The effects of RyR3 deletion were not confined to the physiological level. Whereas the general behavior in the open-field was not different between mutant and control mice, $RyR3^{-/-}$ mice displayed a higher speed of locomotion with a mild tendency for circular running, which extends previous findings of Takeshima *et al.* (1996). Whether these motor alterations result from a dysfunction of the caudate putamen, one of the preferential expression sites of RyR3 in the CNS (Furuichi *et al.*, 1994; Giannini *et al.*, 1995), remains to be investigated. In any case, the unaltered within-session habituation of activity and normal center-field exploration rather argue against emotional alterations or hippocampal dysfunction as underlying causes.

In the knowledge of the distinct deficits in hippocampal synaptic plasticity, it was tempting to test whether they are accompanied by changes in hippocampus-dependent spatial learning. In the acquisition phase and probe trial of the water-maze task, the mutants were rather inconspicuous, i.e. they were able to build and memorize a spatial

map based on a set of distant cues, and use that map to navigate to a hidden platform. This ability depends on synaptic plasticity in the hippocampus and its preservation is in accordance with the normal robust LTP in CA1 and the dentate gyrus. However, the reversal phase of our water-maze experiments revealed that RyR3 mice have a reduced flexibility to reuse and modify an acquired map once the goal position is changed in an otherwise unaltered environment. During relearning, their learning curve resembles that usually observed in a completely new setup, indicating that hippocampal function may not be entirely normal in these mice. The latter finding may be related to the inability of RyR3 knockout mice to maintain weak forms of potentiation induced either by weak tetanic stimulation or by low frequency DP of a robust LTP. Improved reversal learning abilities have been observed in mice overexpressing the cell adhesion molecule L1 (Wolfer *et al*., 1998). In the future, it would be interesting to analyze whether these transgenic mice can rescue the defect of $RyR3^{-/-}$ knockout mice.

In reviewing the results of our experiment, the question arises of how the deletion of the RyR3 isoform may cause such distinct and marked physiological changes. It is reasonable to expect that distinct isoforms could (i) be coupled to different mechanisms of activation and/or (ii) create an interactive mechanism where RyR channels made from one isoform may recruit or interact with RyR channels made from a distinct isoform. RyR3 channels have been estimated to be only ~1–3% of total brain RyR channels (Murayama and Ogawa, 1996). Recent reports on the functional properties of RyR3 channels have shown that a distinctive property is their low sensitivity to inactivation at high calcium concentration (Chen *et al*., 1997; Murayama and Ogawa, 1997; Sonnleitner *et al*., 1998). Such a property would make the RyR3 channels particularly adept at providing a more substained calcium release efflux from the endoplasmic reticulum following stimulation by increasing concentration of calcium mediated by other calcium release channels on the endoplasmic reticulum, or by calcium channels on the plasma membrane (Berridge, 1998). Thus, it can be inferred that the observed impairment of neuronal functions and behavioral defects in RyR3 knockout mice could result from a qualitative contribution of the RyR3 channels to the machinery controlling intracellular calcium levels in neurons. It is interesting to note that these findings closely resemble those reported for neonatal skeletal muscles of RyR3 knockout mice (see Bertocchini *et al*., 1997; Sorrentino and Reggiani, 1999).

Evaluated together, our data suggest a functional role of RyR3 in special forms of hippocampal synaptic plasticity, which might be required for the normal adaptation and modification of spatial maps. In a more general sense, RyR3 seems to be involved in a process that adapts the acquired memory flexibility to external (environmental) changes or stimuli. Recent findings indicate that external changes, such as a novel environment, appetitive or aversive behavioral stimuli, can dramatically influence (reinforce, depotentiate or reverse) a recent potentiation in the hippocampus of freely moving rats (Seidenbecher *et al*., 1997; Xu *et al*., 1998). Since such stimuli directly or indirectly affect learning in most of the learning paradigms (and in real life), conversions between different forms of synaptic plasticity can be suggested to be rather common, and the ability to conduct such changes would appear to be crucial. Hence, the specific deficits in LTP and DP, as well as the reduced flexibility in spatial relearning, support a distinct role for the RyR3 isoform of Ca^{2+} release channels in the regulation of neuronal plasticity.

Materials and methods

Mutant mouse generation and characterization

The method of generation of $RyR3^{-/-}$ knockout mice has been described elsewhere (Bertocchini *et al*., 1997). Mutant ($RyR3^{-/-}$) and normal ($RyR3^{+/+}$) mice were obtained by mating mice heterozygous at RyR3 (i.e. $RyR3^{+/-}$). The genotype of all mice was confirmed by Southern blot analysis of the RyR3 locus (Bertocchini *et al*., 1997). Microsomes were prepared as described previously (Conti *et al*., 1996). Tissues were homogenized in ice-cold buffer A (320 mM sucrose, 5 mM Na–HEPES pH 7.4 and 0.1 mM phenylmethylsulfonyl fluoride) using a Dounce homogenizer. Homogenates were centrifuged at 7000 *g* for 5 min at 4°C. The supernatant obtained was centrifuged at 100 000 *g* for 1 h at 4°C. The microsomes were resuspended in buffer A and stored at –80°C. Protein concentration of the microsomal fraction was quantified using the Bradford protein assay kit (Bio-Rad). Microsomal proteins were separated by SDS–PAGE, transferred to a nitrocellulose membrane (Schleicher & Schuell) and incubated with isoform-specific polyclonal rabbit antisera against the three RyRs. Antigen detection was performed using the alkaline phosphatase detection method (Giannini *et al*., 1995).

Morphological and immunocytochemical investigations

Brain hemispheres were fixed with 4% paraformaldehyde in 0.1 M phosphate-buffered saline (PBS) pH 7.4 overnight, and cut into 60-μm-thick sagittal sections on a vibratome. Slices including the dorsal hippocampus were either processed for Nissl staining or immunocytochemically stained using a standard peroxidase (POD) staining protocol with one of the following primary antibodies: parvalbumin (PV) (clone: PA-235, dilution 1:5000, Sigma), calbindin (CB) (clone: CL-300, dilution 1:5000, Sigma), calretinin (CR) (polyclonal rabbit, dilution 1:5000, Swant) or S100β (polyclonal rabbit, dilution 1:10000, Swant). The incubation time within the primary antisera (including 0.1% Triton X-100) was 36 h at room temperature. Following thorough washing steps in PBS, sections were incubated in goat anti-mouse (PV, CB) or goat anti-rabbit (CR, S100β) biotin (dilution 1:200) for 90 min and visualized by a Vectarstain elite kit (Vector) with DAB as chromophore. Evaluation of the Nissl- and POD-stained sections was performed with a Leica DMRXE microscope. Micrographs were taken with a PL Fluotar 5×, NA 0.12 or PL Fluotar 40× oil, NA 1.0–0.5 objective.

For quantification of Nissl stained sections and S100β-immunoreactive neurons, the CA1 region was divided into subfields by projecting a grid of 10 × 10 divisions over the dorsal hippocampus with the help of a diapositive overlay device that was mounted to the microscope. The grid was centered over CA1 at roughly equal medio-lateral levels and covered an area of 0.42 mm × 0.42 mm = 0.1764 mm^2 in the case of S100β (10 × 10 divisions, including stratum oriens, stratum pyramidale and stratum radiatum; see Figure 2D) or 0.09 mm × 0.03 mm = 0.0027 mm^2 in the case of Nissl-stained sections (10 × 3 divisions over str. pyramidale; see Figure 2B). Cell counts of S100β-positive cells were carried out in three animals per group (five adjacent sections per animal) using a Plan Apo 20x, NA 0.6 objective, zoom factor 1.2, and subsequently calculated for 1 mm^2. Cell counts of the Nissl-stained sections were carried out in three animals per group (15 sections per animal) using a Plan Apo 100× oil, NA 1.4 objective, zoom factor 1.2, and calculated for 1 mm^2.

Electrophysiological recordings

Electrophysiological recordings were conducted as described previously (Frey *et al*., 1988, 1996; Walther *et al*., 1998). For recordings in the CA1 region, slices were maintained in an interface chamber at 32°C for ~5 h of preincubation (ACSF flow rate of 1 ml/min). Two monopolar, lacquer-coated, stainless-steel electrodes were then positioned into different sublayers of the stratum radiatum to stimulate two separate inputs to the same population of pyramidal cells. For recording, two electrodes were positioned in the CA1 dendritic and cell body layer, respectively, to monitor the fEPSP and population spike. The stimulation strength was adjusted such that the population spike attained an amplitude of

25% of the maximum of an input–output (I/O) curve. Once stable responses were obtained for 60 min, LTP was induced in one input by either a 'weak' or a 'strong' tetanization protocol. The weak tetanization protocol consisted of 21 biphasic pulses at 100 Hz (duration 0.2 ms per polarity), and the strong tetanization protocol of three stimulus trains of 100 pulses at 100 Hz, with a 10 min intertrain interval (duration 0.2 ms per polarity). Whilst the weak tetanization paradigm generates a protein-synthesis-independent decremental potentiation under most circumstances, the strong protocol was shown to induce protein-synthesis-dependent late-LTP (Frey *et al*., 1988; Frey and Morris, 1997). LTP was recorded for at least 2 h using the weak tetanization protocol and at least 6 h applying the strong protocol.

Recording in the dentate gyrus was performed similarly to that in CA1. The slices were kept in a 'submerged type' chamber and a monopolar, lacquer-coated, stainless-steel electrode was placed in the stratum moleculare of the dentate gyrus to stimulate the medial perforant path input, which was distinguished by its localization and the presence of paired-pulse depression of fEPSP at an interpulse interval of 40 ms. About 200 μm apart, the recording electrode was lowered to the same level to record fEPSPs. The stimulation voltage was adjusted to elicit a fEPSP slope of 35% of the maximum of the corresponding I/O curve. LTP was induced by a repeated, 3-fold tetanization paradigm consisting of 15 bursts of eight pulses, 200 Hz, interburst interval 200 ms, which were applied with an interval of 10 min. For examination of DP, LTP was generated by a single tetanization consisting of 15 bursts of four pulses, 100 Hz, interburst interval 200 ms. Five minutes after tetanization, potentiation was reversed by a 2 min train of low-frequency stimulation at 5 Hz. To check paired-pulse depression (PPD), three paired-pulses with interpulse intervals of 10, 40, 100, 200 and 500 ms were delivered at 60 s intervals at a stimulation voltage adjusted to 35% of the maximum. The three responses were averaged and the degree of PPD was defined as % PPD (fEPSP slope 2nd pulse×100/fEPSP slope 1st pulse).

To allow a direct comparison, the recording of slices from mutant mice was interleaved with experiments with wild-type controls. Statistical analysis was performed using the two-tailed Mann–Whitney U-test, the Wilcoxon matched-pairs signed rank test or a non-parametric ANOVA (Friedman test).

Behavioral studies

For open-field recording, the water was removed from our swimming navigation pool and a white plastic floor was inserted at the level of the water surface. The subject was introduced into the arena next to the side wall and its activity was recorded for 10 min by the video camera. *x–y* coordinates were extracted at a frequency of 4.2 Hz and with 256 × 256 pixels of spatial resolution. A second session was recorded on the following day. In order to assess within-session changes of activity, both recording sessions were divided into two 5 min observation periods. Locomotor activity was assessed by the total distance traveled (m) and by the percentage of active time (locomotion speed >0.06 m/s). For the calculation of the average speed of locomotion, periods of inactivity were excluded. In order to obtain an estimate of circular running tendency, a circling bias was determined as follows. The coordinate stream was subdivided into periods of immobility, straight segments and curves with consistent change of direction, and the direction changes of all curves (degrees, clockwise = negative, counter-clockwise = positive) were summed. The absolute value of the sum served as a measure for circular running. Thigmotaxis and center exploration were quantified by determining the time spent within 9 cm of the wall (wall contact zone) and in the center field of 1.1 m diameter, respectively. Statistical analysis of open-field parameters was done using two-way analysis of variance with genotype as the between-subjects factor and observation as the within-subject factor.

The swimming navigation set-up followed the description given by Morris (1984). A white Plexiglas circular pool of 150 cm diameter and 50 cm height was filled with water (16 cm deep, 24–26°C) made opaque by the addition of milk. Distant visual cues for navigation were available on the walls of the room illuminated by diffuse light (12 lux). A wire mesh platform (16 × 16 cm) was placed 0.5 cm below the water surface, at 35 cm from the wall of the pool. To avoid visual orientation prior to release, the mice were transferred from their cages to the pool in an opaque plastic cup. They were released from eight symmetrically placed positions on the pool perimeter in a predetermined but not sequential order. The mice were allowed to swim until they found the platform or until 120 s had elapsed. Between trials, the animals were placed under red lamps and allowed to warm up and dry off for a few minutes. Intertrial times varied from 30 to 60 min. The entire procedure took 5 days; each animal performed a total of 30 trials, 6 per day. The position of the hidden platform remained fixed for the first 3 days (18 trials, acquisition phase). Afterwards, it was placed in the opposite quadrant for 2 days (12 trials, reversal phase). The first 60 s of the first reversal trial served as probe trial to analyze spatial retention and search behavior of the animals. Swim paths were recorded by a video camera and fed to an electronic imaging system (Noldus EthoVision version 1.96) that extracted and stored *x–y* coordinates at a frequency of 4.2 Hz and with 256 × 256 pixels of spatial resolution. The coordinates were analyzed offline using WinTrack 2.0. An earlier version of this custom software has been described in detail elsewhere (Wolfer and Lipp, 1992). Escape performance was judged by escape time, length of swim path and the cumulative search error according to Gallagher *et al*. (1993). Motor patterns were measured by assessing swim speed (m/s) while moving faster than 6 cm/s and by determining the percentage of time spent floating (defined as speed below 6 cm/s). Circling tendency was assessed in the same way as in the open-field. For statistical analysis of performance during acquisition, parameters were averaged over blocks of two trials and subjected to two-way ANOVA with genotype as the between-subjects factor and trial block as the within-subject factor. Probe trial performance (first 60 s of first reversal trial) was assessed by the percentage of time spent in the former target versus adjacent quadrants, and by the number of annulus crossings over the former versus adjacent target positions. Probe trial parameters were evaluated statistically by two-way ANOVA including genotype as the between-subjects factor and place (former goal versus average of adjacent quadrants) as the within-subject factor. When comparing the acquisition with the reversal phase as a whole, parameters were averaged over all trials of acquisition and reversal, respectively, and subjected to two-way ANOVA with genotype as the between-subjects factor and phase as the within-subject factor. *Post hoc* comparisons were made using the Scheffe test.

Acknowledgements

The excellent technical assistance of Sabine Hartmann, Diana Koch and Marijana Stagliar is gratefully acknowledged. This work was supported by grants from the Deutsche Forschungsgemeinschaft (SFB 42602) to J.U.F., Human Frontier Science Program to H.P.L., and Telethon (1151), EEC (96-0656) and Murst 1998 to V.S..

References

Alcazar,A., Martin de la Vega,C., Bazan,E., Fando,J.L. and Salinas,M. (1997) Calcium mobilization by ryanodine promotes the phosphorylation of initiation factor 2α subunit and inhibits protein synthesis in cultured neurons. *J. Neurochem.*, **69**, 1703–1708.

Alkon,D.L., Nelson,T.J., Zhao,W. and Cavallaro,S. (1998) Time domains of neuronal Ca^{2+} signaling and associative memory: steps through a calexcitin, ryanodine receptor, K^+ channel cascade. *Trends Neurosci.*, **21**, 529–537.

Anderson,P. (1960) Interhippocampal impulses. *Acta Physiol. Scand.*, **48**, 178–480.

Artola,A. and Singer,W. (1993) Long-term depression of excitatory synaptic transmission and its relationship to long-term potentiation. *Trends Neurosci.*, **16**, 480–487.

Barrionuevo,G., Schottler,F. and Lynch,G. (1980) The effects of repetitive low frequency stimulation on control and 'potentiated' synaptic responses in the hippocampus. *Life Sci.*, **27**, 2385–2391.

Berridge,M.J. (1998) Neuronal calcium signaling. *Neuron*, **21**, 13–26.

Bertocchini,F., Ovitt,C., Conti,A., Barone,V., Scholer,H.R., Reggiani,C. and Sorrentino,V. (1997) Requirement of the ryanodine receptor type 3 for efficient contraction in neonatal skeletal muscles. *EMBO J.*, **16**, 6956–6963.

Bliss,T.V.P. and Collingridge,G.L. (1993) A synaptic model of memory: long-term potentiation in the hippocampus. *Nature*, **361**, 31–39.

Bootman,M.D. and Berridge,M.J. (1995) The elemental principles of calcium signaling. *Cell*, **83**, 675–678.

Chavis,P., Fagni,L., Lansman,J.B. and Bockaert,J. (1996) Functional coupling between ryanodine receptors and L-type calcium channels in neurons. *Nature*, **382**, 719–722.

Chen,W.S.R., Li,X., Ebisawa,K. and Zhang,L. (1997) Functional characterization of the recombinant type 3 Ca^{2+} release channel (ryanodine receptor) expressed in HEK293 Cells. *J. Biol. Chem.*, **272**, 24234–24246.

Conti,A., Gorza,L. and Sorrentino,V. (1996) Differential distribution of ryanodine receptor type 3 (RyR3) gene product in mammalian skeletal muscles. *Biochem. J.*, **316**, 19–23.

Cummings,J.A., Mulkey,R.M., Nicoll,R.A. and Malenka,R.C. (1996) Ca^{2+} signaling requirements for long-term depression in the hippocampus. *Neuron*, **16**, 825–833.

Curtis,D.R. and Eccles,J.C. (1960). Synaptic action during and after repetitive stimulation. *J. Physiol. (Lond.)*, **183**, 341–359.

Davis,H.P. and Squire,L.R. (1984) Protein synthesis and memory. *Psychol. Bull.*, **96**, 518–559.

Doyere,V., Srebro,B. and Laroche,S. (1997) Heterosynaptic LTD and depotentiation in the medial perforant path of the dentate gyrus in the freely moving rat. *J. Neurophysiol*., **77**, 571–578.

Flucher,B.E., Conti,A., Takeshima,H. and Sorrentino,V. (1999) Type 3 and Type 1 ryanodine receptors are localized in triads of the same mammalian skeletal muscle fibers. *J. Cell Biol*., **146**, 621–630.

Frenguelli,B.G., Irving,A.J. and Collingridge,G.L. (1996) Ca^{2+} stores and hippocampal synaptic plasticity. *Semin. Neurosci*., **8**, 301–309.

Frey,U. and Morris,R.G.M. (1997) Synaptic tagging and long-term potentiation. *Nature*, **385**, 533–536.

Frey,U., Krug,M., Reymann,K.G. and Matthies,H. (1988) Anisomycin, an inhibitor of protein synthesis, blocks late phases of LTP phenomena in the hippocampal CA1 region *in vitro*. *Brain Res*., **452**, 57–65.

Frey,U., Müller,M. and Kuhl,D. (1996) A different form of long-lasting potentiation revealed in tissue plasminogen activator mutant mice. *J. Neurosci*., **16**, 2057–2063.

Furuichi,T., Furutama,D., Hakamata,Y., Nakai,J., Takeshima,H. and Mikoshiba,K. (1994) Multiple types of ryanodine receptor/Ca^{2+} release channels are differentially expressed in rabbit brain. *J. Neurosci.*, **14**, 4794–4805.

Gallagher,M., Burwell,R. and Burchinal,M. (1993) Severity of spatial learning impairment in aging: development of a learning index for performance in the Morris water maze. *Behav. Neurosci.*, **107**, 618–626.

Giannini,G., Conti,A., Mammarella,S., Scrobogna,M. and Sorrentino,V. (1995) The ryanodine receptor/calcium channel genes are widely and differentially expressed in murine brain and peripheral tissues. *J. Cell Biol*., **128**, 893–904.

Goelet,P., Castellucci,V.F., Schacher,S. and Kandel,E.R. (1986) The long and the short of long-term memory—a molecular framework. *Nature*, **322**, 419–422.

Grover,L.M. and Teyler,T.J. (1990) Two components of long-term potentiation induced by different patterns of activation. *Nature*, **347**, 477–479.

Grover,L.M. and Teyler,T.J. (1994) Activation of NMDA receptors by low and high frequency orthodromic stimulation and their contribution to induction of long-term potentiation. *Synapse*, **16**, 66–75.

Kohda,K., Inoue,T. and Mikoshiba,K. (1995) Ca^{2+} release from Ca^{2+} stores, particularly from ryanodine-sensitive Ca^{2+} stores, is required for the induction of LTD in cultured cerebellar Purkinje cells. *J. Neurophysiol*., **74**, 2184–2188.

Lisman,J. (1989) A mechanism for the Hebb and the anti-Hebb processes underlying learning and memory. *Proc. Natl Acad. Sci. USA*, **86**, 9574–9578.

Malenka,R.C., Kauer,J.A., Zucker,R.J. and Nicoll,R.J. (1988) Post-synaptic calcium is sufficient for potentiation of hippocampal synaptic transmission. *Science*, **242**, 81–84.

Malenka,R.C., Lancaster,B. and Zucker,R.S. (1992) Temporal limits on the rise in postsynaptic calcium required for the induction of long-term potentiation. *Neuron*, **9**, 121–128.

Matthies,H. (1989) In search of the cellular mechanisms of memory. *Prog. Neurobiol*., **32**, 277–349.

McNaughton,B.L. (1982) Evidence for two physiologically distinct perforant pathways to the fascia dentata. *Brain Res.*, **199**, 1–19.

Morris,R.G.M. (1984) Developments of a water-maze procedure for studying spatial learning in the rat. *J. Neurosci. Methods*, **11**, 47–60.

Murayama,T. and Ogawa,Y. (1996) Properties of RyR3 ryanodine receptor isoform in mammalian brain. *J. Biol. Chem.*, **271**, 5079–5084.

Murayama,T. and Ogawa,Y. (1997) Characterization of type 3 Ryanodine receptor (RyR3) in mammalian diaphragm muscle. *J. Biol. Chem.*, **272**, 24030–24037.

Neveau,D. and Zucker,R.S. (1996) Postsynaptic levels of calcium needed to trigger LTD and LTP. *Neuron*, **16**, 619–629.

O'Mara,S.M, Rowan,M.J. and Anwyl,R. (1995) Dantrolene inhibits long-term depression and depotentiation of synaptic transmission in the rat dentate gyrus. *Neuroscience*, **68**, 621–624.

Reyes,M. and Stanton,P.K. (1996) Induction of hippocampal long-term depression requires release of Ca^{2+} from separate presynaptic and postsynaptic intracellular stores. *J. Neurosci.*, **16**, 5951–5960.

Reyes-Harde,M., Empson,R., Potter,B.V.L., Galione,A. and Stanton,P.K. (1999) Evidence of a role for cyclic ADP-ribose in long-term synaptic depression in hippocampus. *Proc. Natl Acad. Sci. USA*, **96**, 4061–4066.

Rosenzweig,M.R. (1996) Aspects of the search for neural mechanisms of memory. *Annu. Rev. Psychol.*, **47**, 1–32.

Seidenbecher,T., Reymann,K.G. and Balschun,D. (1997) A post-tetanic time window for the reinforcement of long-term potentiation by appetitive and aversive stimuli. *Proc. Natl Acad. Sci. USA*, **94**, 1494–1499.

Sharp,A.H., McPherson,P.S., Dawson,T.M., Aoki,C., Campbell,K.P. and Snyder,S.H. (1993) Differential immunohistochemical localization of inositol, 1,4,5,-trisphosphate- and ryanodine-sensitive Ca^{2+} release channels in rat brain. *J. Neurosci.*, **13**, 3051–3063.

Sonnleitner,A., Conti,A., Bertocchini,F., Schindler,H. and Sorrentino,V. (1998) Functional properties of the Ryanodine receptor type 3 (RyR3) Ca^{2+} release channel. *EMBO J*., **17**, 2790–2798.

Sorrentino,V. and Reggiani,C. (1999) Expression of Ryanodine receptor type 3 in skeletal muscle: a new partner in excitation-contraction coupling? *Trends Cardiovasc. Med.*, **9**, 53–60.

Stäubli,U. and Chun,D. (1996) Factors regulating the reversibility of long-term potentiation. *J. Neurosci.*, **16**, 853–860.

Takeshima,H. *et al*. (1996) Generation and characterization of mutant mice lacking Ryanodine receptor type 3. *J. Biol. Chem.*, **271**, 19649–19652.

Tsumoto,T. and Yasuda,H. (1996) A switching role of postsynaptic calcium in the induction of long-term potentiation or long-term depression in visual cortex. *Semin. Neurosci*., **8**, 311–319.

Wagner,J.J. and Alger,B.E. (1996) Homosynaptic LTD and depotentiation: do they differ in name only? *Hippocampus*, **6**, 24–29.

Walther,T., Balschun,D., Voigt,J.-P., Fink,H., Zuschratter,W., Birchmeier, C., Ganten,D. and Bader,M. (1998) Sustained long-term potentiation and anxiety in mice lacking the *Mas* protooncogene. *J. Biol. Chem.*, **19**, 11867–11873.

Wang,Y., Wu,J., Rowan,M.J. and Anwyl,R. (1996) Ryanodine produces a low frequency stimulation-induced NMDA receptor-independent long-term potentiation in the rat dentate gyrus *in vitro*. *J. Physiol.*, **495**, 755–767.

Wang,Y., Rowan,M.J. and Anwyl,R. (1997) Induction of LTD in the dentate gyrus *in vitro* is NMDA receptor independent, but dependent on Ca^{2+} influx via low-voltage-activated Ca^{2+} channels and release of Ca^{2+} from intracellular stores. *J. Neurophysiol*., **77**, 812–825.

Wilsch,V.W., Behnisch,T., Jäger,T., Reymann,K.G. and Balschun,D. (1998) When are class I metabotropic glutamate receptors necessary for long-term potentiation? *J. Neurosci*., **18**, 6071–6080.

Wolfer,D.P. and Lipp,H.-P. (1992) A new computer program for detailed off-line analysis of swimming navigation in the Morris water maze. *J. Neurosci. Methods*, **41**, 65–74.

Wolfer,D.P., Mohajeri,H.M., Lipp,H.P. and Schachner,M. (1998) Increased flexibility and selectivity in spatial learning of transgenic mice ectopically expressing the neural cell adhesion molecule L1 in astrocytes. *Eur. J. Neurosci.*, **10**, 708–717.

Xu,L., Anwyl,R. and Rowan,M.J. (1998) Spatial exploration induces a persistent reversal of long-term potentiation in rat hippocampus. *Nature*, **394**, 891–894.

Xu,Y.Z. and Krnjevic,K. (1990) Induction of long-term potentiation in isolated slices of Sprague-Dawley rat hippocampus is not blocked by dantrolene sodium. *J. Physiol.*, **426**, 50.

Received May 26, 1999; revised and accepted August 5, 1999